Swelling-activated Gd^{3+}-sensitive Cation Current and Cell Volume Regulation in Rabbit Ventricular Myocytes

Henry F. Clemo*‡ and Clive M. Baumgarten‡

From the *Department of Internal Medicine (Cardiology), and ‡Department of Physiology, Medical College of Virginia, Virginia Commonwealth University, Richmond, Virginia 23298

abstract The role of swelling-activated currents in cell volume regulation is unclear. Currents elicited by swelling rabbit ventricular myocytes in solutions with 0.6–0.9× normal osmolarity were studied using amphotericin perforated patch clamp techniques, and cell volume was examined concurrently by digital video microscopy. Graded swelling caused graded activation of an inwardly rectifying, time-independent cation current ($I_{Cir,swell}$) that was reversibly blocked by Gd^{3+}, but $I_{Cir,swell}$ was not detected in isotonic or hypertonic media. This current was not related to I_{K1} because it was insensitive to Ba^{2+}. The P_K/P_{Na} ratio for $I_{Cir,swell}$ was 5.9 ± 0.3, implying that inward current is largely Na^+ under physiological conditions. Increasing bath K^+ increased $g_{Cir,swell}$ but decreased rectification. Gd^{3+} block was fitted with a $K_{0.5}$ of 1.7 ± 0.3 μM and Hill coefficient, n, of 1.7 ± 0.4. Exposure to Gd^{3+} also reduced hypotonic swelling by up to ~30%, and block of current preceded the volume change by ~1 min. Gd^{3+}-induced cell shrinkage was proportional to $I_{Cir,swell}$ when $I_{Cir,swell}$ was varied by graded swelling or Gd^{3+} concentration and was voltage dependent, reflecting the voltage dependence of $I_{Cir,swell}$. Integrating the blocked ion flux and calculating the resulting change in osmolarity suggested that $I_{Cir,swell}$ was sufficient to explain the majority of the volume change at –80 mV. In addition, swelling activated an outwardly rectifying Cl^- current, $I_{Cl,swell}$. This current was absent after Cl^- replacement, reversed at E_{Cl}, and was blocked by 1 mM 9-anthracene carboxylic acid. Block of $I_{Cl,swell}$ provoked a 28% increase in swelling in hypotonic media. Thus, both cation and anion swelling-activated currents modulated the volume of ventricular myocytes. Besides its effects on cell volume, $I_{Cir,swell}$ is expected to cause diastolic depolarization. Activation of $I_{Cir,swell}$ also is likely to affect contraction and other physiological processes in myocytes.

key words: osmoregulation • stretch-activated channels • mechano-electrical feedback • arrhythmias

introduction

Ion channels activated by mechanical stretch or cell swelling (SAC)[1] are present in cells ranging in complexity from primitive unicellular organisms to highly differentiated neurons and myocytes (Sachs, 1988; Morris, 1990; Sackin, 1995; Sukharev et al., 1996; Vandenberg et al., 1996). Members of this class of channels exhibit varying selectivity, conductance, kinetics, and requirements for activation. In cardiac myocytes, for example, osmotic or hydrostatic pressure-induced cell swelling activates Cl^- channels (Tseng, 1992; Sorota, 1992; Hagiwara et al., 1992; Coulombe and Coraboeuf, 1992; Zhang et al., 1993), and mechanical deformation or swelling activate both poorly selective cation (Craelius, 1988; Bustamante et al., 1991; Sigurdson et al., 1992; Sadoshima et al., 1992; Kim, 1993; Kim and Fu, 1993; Ruknudin et al., 1993) and K^+-selective channels (Brezden et al., 1986; Kim, 1992; Sasaki et al., 1992; Van Wagoner, 1993; Ruknudin et al., 1993).

The broad distribution of SACs suggests their sensitivity to mechanical stretch or swelling must subserve fundamental cellular functions or reflect fundamental properties of ion channels. One appealing physiological role is in cell volume regulation. After rapid swelling on exposure to hypotonic media, activation of transport pathways allows many cell lines to normalize their volume in a process called a regulatory volume decrease (RVD). SACs have been implicated in the RVD observed in Ehrlich ascites tumor cells (Lambert and Hoffman, 1994), renal cortical duct cells (Schwiebert et al., 1994), and embryonic chick cardiac myocytes (Rasmusson et al., 1993; Zhang et al., 1993). In contrast, rabbit myocytes can swell significantly without an RVD (Drewnowska and Baumgarten, 1991; Suleymanian and Baumgarten, 1996).

To investigate whether SACs regulate cell volume in mammalian cardiac myocytes, Suleymanian et al. (1995) used Gd^{3+} and 9-anthracene carboxylic acid (9-AC) as markers of channel activity. Gd^{3+} blocks stretch-activated, poorly selective cation channels (Yang and Sachs, 1989; Sadoshima et al., 1992; Hamill and McBride, 1996), and 9-AC blocks swelling-activated Cl^- channels

Address correspondence to Dr. C.M. Baumgarten, Department of Physiology, Box 980551, Medical College of Virginia, Richmond, VA 23298-0551. FAX: 804-828-7382; E-mail: baumgart@gems.vcu.edu

[1] *Abbreviations used in this paper:* 9-AC, 9-anthracene carboxylic acid; E_h, holding potential; I-V, current-voltage; NMDG, *N*-methyl-D-glucamine; RVD, regulatory volume decrease; SAC, stretch- or swelling-activated channel.

J. Gen. Physiol. © The Rockefeller University Press • 0022-1295/97/09/297/16 $2.00
Volume 110 September 1997 297–312
http://www.jgp.org

(Tseng, 1992; Sorota, 1992, 1994; Hagiwara, 1992; Vandenberg et al., 1994). Under physiological osmotic conditions, when SACs presumably are silent, neither blocker alters the volume of isolated rabbit ventricular cells. In hypotonic solutions, however, Gd^{3+} significantly decreases and 9-AC significantly increases rabbit ventricular myocyte volume (Suleymanian et al., 1995). These data on intact, unclamped cells were explained by suggesting that osmotic swelling activates Gd^{3+} and 9-AC–sensitive ion channels that mediate sustained cation and anion fluxes, respectively, and in turn modulate cell volume.

Volume regulation in cultured chick myocytes appears to be different than in freshly isolated rabbit myocytes. Chick heart cells exhibit a strong RVD in response to osmotic swelling that is attenuated by removing Cl^- (Rasmusson et al., 1993). Osmotic and hydrostatic swelling is sustained and activates a Gd^{3+}-sensitive Cl^- current during ruptured patch whole-cell recordings (Zhang et al., 1993; Zhang and Lieberman, 1996). These workers concluded, however, that the swelling-induced Cl^- current does not contribute to regulation of chick heart cell volume because a complete RVD occurred and a Cl^- current was not generated under perforated patch conditions (Hall et al., 1995). This emphasizes that ruptured patch techniques may distort cell volume regulation.

The present work describes a swelling-induced, Gd^{3+}-sensitive current in rabbit ventricular myocytes and examines its role in cell volume regulation. The perforated patch voltage-clamp technique and video microscopy were used to simultaneously determine whole-cell ionic currents and the relative cell volume in the absence and presence of osmotic swelling. The experiments demonstrated that: (*a*) osmotic swelling elicited a graded, inwardly rectifying, Gd^{3+}-sensitive cation current, termed $I_{Cir,swell}$, that could be separated from an outwardly rectifying, 9-AC–sensitive anion current, $I_{Cl,swell}$; (*b*) $I_{Cir,swell}$ poorly distinguishes between K^+ and Na^+; (*c*) block of $I_{Cir,swell}$ by Gd^{3+} reduces the volume of osmotically swollen cells in a swelling- and voltage-dependent manner; and (*d*) the magnitude of the Gd^{3+}-sensitive current can largely account for the Gd^{3+}-induced cell shrinkage. A preliminary report appeared previously (Clemo and Baumgarten, 1995).

MATERIALS AND METHODS

Cell Isolation

Ventricular myocytes were freshly isolated from New Zealand white rabbits (2.5–3 kg) using a collagenase–pronase dispersion method as previously described (Clemo and Baumgarten, 1991; Clemo et al., 1992). Cells were stored in a modified Kraft-Brühe solution containing (mM): 132 KOH, 120 glutamic acid, 2.5 KCl, 10 KH_2PO_4, 1.8 $MgSO_4$, 0.5 K_2EGTA, 11 glucose, 10 taurine, 10 HEPES (pH 7.2, 295 mosm/liter). Typical yields were 50–70% Ca^{2+}-tolerant, rod-shaped cells. Myocytes were used within 6 h of harvesting, and only quiescent cells with no evidence of membrane blebbing were selected for study.

Experimental Solutions

Cells were placed in a glass-bottomed chamber (~0.3 ml) and superfused with room temperature (21–22°C) bathing solution at 3 ml/min. Solution changes were complete within 10 s, as estimated from the liquid junction potential of a microelectrode. The standard bathing solution contained (mM): 65 NaCl, 5 KCl, 2.5 $CaSO_4$, 0.5 $MgSO_4$, 5 HEPES, 10 glucose, and 17–283 mannitol (pH 7.4). The reduced, fixed NaCl concentration permitted adjustment of osmolarity with mannitol at a constant ionic strength. An osmolarity of 296 mosm/liter was taken as isotonicity (1T). Osmolarity ranged from 178 to 266 mosm/liter in hypotonic solutions (0.6T–0.9T) and was 444 mosm/liter in hypertonic solution (1.5T). Osmolarity routinely was verified with a freezing-point depression osmometer (Osmette S; Precision Systems Inc., Natick, MA).

To evaluate the roles of specific ions, nominally Ca^{2+}-free, Na^+-, K^+-, and Ca^{2+}-free, and Cl^-- and Ca^{2+}-free solutions were prepared. $MgSO_4$ replaced $CaSO_4$, *N*-methyl-D-glucamine (NMDG) Cl replaced NaCl and KCl, or Na and K methanesulfonate replaced NaCl and KCl on equimolar bases.

Voltage Clamp

Electrodes were pulled from 7740 glass capillary tubing (1.5 mm o.d., 1.12 mm i.d., filament; Glass Co. of America, Bargaintown, NJ) to give a final tip diameter of 3–4 μm and a resistance of 0.5–1 MΩ. The standard electrode filling solution contained (mM): 120 K aspartate, 10 KCl, 10 NaCl, 3 $MgSO_4$, 10 HEPES, pH 7.1. In addition, a Na^+- and K^+-free pipette solution was made by replacing Na^+ and K^+ salts with Cs^+ salts, and a low Cl^- (5 mM) pipette solution was made by replacing NaCl and KCl with the corresponding aspartate salts.

Whole-cell currents were measured using an Axoclamp 200A amplifier (Axon Instruments, Inc., Foster City, CA). Pulse and ramp protocols, voltage-clamp data acquisition, and off-line data analysis were controlled with custom programs written in ASYST (Keithley, Taunton, MA). Both step and ramp voltage-clamp protocols were applied (see Fig. 1, *D* and *G*), and holding potential (E_h) was either −80, −40, or 0 mV. In step protocols, the test voltage step was 500 ms in duration. Current during the last 50 ms of the step was averaged and called steady state current. In ramp protocols, the voltage was stepped from E_h to +40 mV for 20 ms, ramped to −100 mV over 5 s, and, after 10 ms, ramped back to +40 mV over 5 s. To cancel the capacitive current, the depolarizing and hyperpolarizing arms of the ramp were averaged. A very slow voltage ramp (28 mV/s) was used so as to approach steady state, and ramp current–voltage (I-V) relationships were in good agreement with those obtained by voltage steps. Nevertheless, the contribution of slowly activating currents such as the slow component of the delayed rectifier, I_{Ks}, may be underestimated. Both step and ramp currents were digitized at 1 kHz and low-pass filtered at 200 Hz. The reported E_m was corrected for the liquid junction potential of the patch electrode as measured from the change in potential upon switching the bath between the superfusing and electrode-filling solutions (Neher, 1992), and the bath was grounded with a 3 M KCl agar bridge.

Perforated Patch Technique

Volume measurements initially were attempted during ruptured-patch voltage clamp, but this approach proved unsuitable. As previously described for both cardiac myocytes (Sorota, 1992) and other cell lines (Worrell et al., 1989; Doroshenko and Neher, 1992; Kinard and Satin, 1995), isosmotic pipette and bath solutions sometimes precipitated unpredictable cell swelling and changes in whole-cell currents. To prevent this problem, the amphotericin perforated patch technique (Horn and Marty, 1988; Rae et al., 1991) was employed. Both cell volume and whole-cell currents were stable under perforated patch recording conditions (Sorota, 1992; Hall et al., 1995).

Amphotericin-B (Sigma Chemical Co., St. Louis, MO) was freshly dissolved in dimethylsulfoxide, and then diluted in electrode filling solution to give final amphotericin and DMSO concentrations of 100 μg/ml and 0.2% (vol/vol), respectively. The electrode tip was dipped into amphotericin-free filling solution for 2 s, and then the barrel was backfilled with amphotericin-containing solution. Filled pipettes were quickly attached to a Ag/AgCl half-cell, placed in the bath solution, and zeroed. Gigaseals were formed without application of negative pressure, typically 30–45 s after backfilling the pipette. To follow the formation of amphotericin pores, access resistance and cell capacitance were monitored with 10-mV hyperpolarizing pulses from E_h. After ~20 min, access resistance fell to 7–10 MΩ, and cell capacitance was 70–200 pF.

The cation/anion permeability ratio of a perforated patch depends on characteristics of both the ionophore and endogenous ion channels. Because the permeability ratio affects the transport numbers for ion fluxes between the pipette and cytoplasm, it may affect the cell volume attained under voltage clamp (see DISCUSSION). The P_K/P_{Cl} ratio of amphotericin-treated cardiac sarcolemma was evaluated by exposing the entire sarcolemma to ionophore and determining the zero current potential under current clamp. For these measurements, the ruptured patch procedure was exploited. Seals were made while myocytes were incubated in a solution containing (mM): 140 KCl, 3 $MgSO_4$, 5 HEPES, 10 glucose, pH 7.4; this represented the pipette filling solution in perforated patch experiments. The ruptured patch electrodes contained (mM): 40 KCl, 85 K aspartate, 3 $MgCl_2$, 5 K_2EGTA, 3 K_2ATP, 10 HEPES, pH 7.1. After exposure to amphotericin (160 μg/ml) in the bath solution, the bath was switched to a series of solutions with varying concentrations of K^+ (1–140 mM, K^+ replaced with NMDG) or Cl^- (1–140 mM, Cl^- replaced with aspartate). The known intracellular and extracellular K^+ and Cl^- concentrations and measured E_m data were fit to the Goldman-Hodgkin-Katz equation (TABLECURVE 2D; SPSS, Chicago, IL). P_K/P_{Cl} was 0.9 ± 0.07 when extracellular Cl^- was varied ($n = 5$) and was 0.8 ± 0.03 when extracellular K^+ was varied ($n = 5$). Because experiments treating the entire sarcolemma with amphotericin could not exactly mimic the perforated patch experiments, these permeability ratios should be regarded as approximate.

Determination of Relative Cell Volume

Methods for determining relative cell volume have been described previously (Clemo and Baumgarten, 1991; Clemo et al., 1992; Suleymanian and Baumgarten, 1996). Myocytes were visualized with an inverted microscope (Diaphot; Nikon Inc., Garden City, NY) equipped with Hoffman modulation optics (40×; 0.55 NA) and a high resolution TV camera (CCD72; Dage-MTI; Michigan City, IN) coupled to a video frame-grabber (Targa-M8; Truevision, Santa Clara, CA). Images were captured on-line each time a ramp or step voltage-clamp protocol was performed by a program written in C and assembler and linked to the ASYST voltage-clamp software. A combination of commercial (MOCHA; SPSS) and custom (ASYST) programs were used to determine cell width, length, and the area of the image.

Changes in cell width and thickness on exposure to anisosmotic solutions are proportional (Drewnowska and Baumgarten, 1991). Using each cell as its own control, relative cell volume was calculated as:

$$\text{volume}_t/\text{volume}_c = (\text{area}_t \times \text{width}_t)\ /\ (\text{area}_c \times \text{width}_c)$$

where t and c refer to test (e.g., 0.6T) and control (1T) solutions, respectively. These methods provide estimates of relative cell volume that are reproducible to within 1% (Clemo and Baumgarten, 1991; Clemo et al., 1992, Suleymanian and Baumgarten, 1996).

Statistics

Data are reported as mean ± SEM; *n* represents the number of cells. Except for Fig. 1, which depicts voltage clamp data from a typical experiment, all I-V relationships are averages, and mean current densities are expressed in pA/pF to account for differences in cell membrane area. When multiple comparisons were made, data were subjected to analysis of variance. Bonferroni's method for group comparisons was performed when appropriate. For simple comparisons, the Student's *t* test was used. All statistical analyses were conducted in SIGMASTAT (SPSS).

RESULTS

Characterization of Stretch-activated Currents

Membrane currents elicited by hyposmotic cell swelling initially were studied by applying step and ramp voltage-clamp protocols to the same cell. Results for a typical cell in standard bath solution are shown in Fig. 1. For the step protocol, E_h was −40 mV, and depolarizations to test potentials between −100 and +40 mV were applied under control conditions (1T, Fig. 1 *A*) and again 5 min after swelling in 0.6T hypotonic solution (Fig. 1 *B*). The currents obtained after osmotic stretch were much larger than those obtained in 1T solution. The effects are depicted more clearly in Fig. 1 *C* in which swelling-induced difference currents, measured as the current in 0.6T minus that in 1T, are plotted. The difference currents were time independent over most of the voltage range explored. Between 0 and +40 mV, however, osmotic stretch provoked an increasing outward current that approached steady state during the 500-ms pulse. This time-dependent current resembles the delayed rectifier, I_K, which is augmented by osmotic and hydrostatic cell swelling of guinea pig myocytes (Sasaki et al., 1992, 1994; Rees et al., 1995; Wang et al., 1996).

After recovery in 1T solution, the same cell was studied using the ramp protocol (28 mV/s) to define the steady state I-V relationship. As before, the currents in 0.6T were larger than those in 1T (Fig. 1 *E*). The I-V relationship for the osmotic stretch-induced difference current (Fig. 1 *F, solid line*) exhibited strong inward rectification at negative potentials and weaker outward rectification at positive potentials. Fig. 1 *F* also compares the results of the two voltage-clamp protocols. Steady state difference currents measured using the step protocol (●, data from Fig. 1 *C*) are superimposed

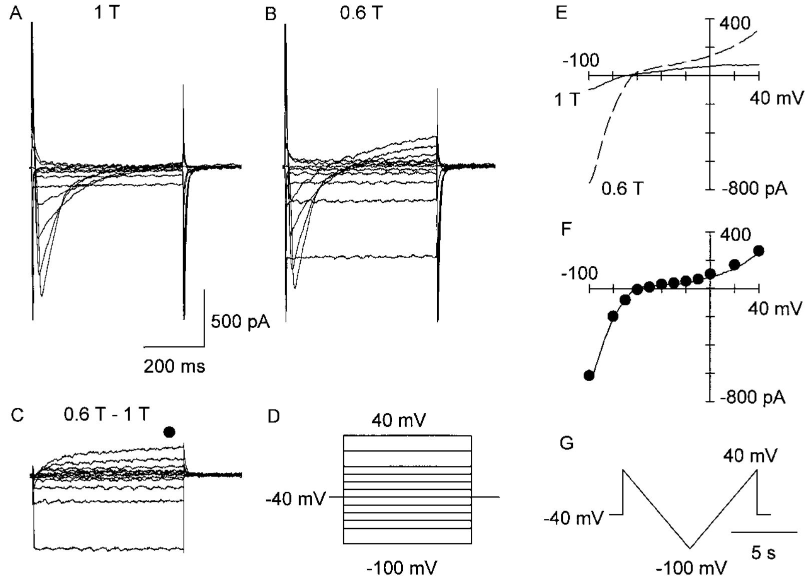

FIGURE 1. Currents activated on cell swelling. Voltage steps were applied to characterize whole-cell currents under isotonic (*A, 1T*) and hypotonic (*B, 0.6T*) conditions. (*C*) Difference currents ($I_{0.6T} - I_{1T}$) for step protocol shown in *D*. Swelling in 0.6T solution increased the currents at the end of 500-ms pulses. (*E*) Same cell studied in 1T and 0.6T solutions with a ramp protocol (28 mV/s). Hypotonic solution induced an inwardly rectifying current at negative potentials and an outwardly rectifying current at positive potentials. (*F*) Difference current elicited with voltage ramps (*solid line*). Steady state step difference currents (●, from *C*) superimpose on ramp difference current. (*G*) Diagram of ramp protocol.

on the difference current obtained with the ramp protocol. The good agreement verifies the adequacy of ramp protocols for determining swelling-induced steady state currents. Ramp clamps were used in subsequent experiments that were designed to study maintained currents that are likely to contribute to cell volume regulation.

Previous work on mammalian cardiac myocytes has described both a Gd^{3+}-sensitive cation channel in cell-attached and excised patches that is activated by pipette suction (Bustamante et al., 1991) or mechanical stretch (Sadoshima et al., 1992) and a Gd^{3+}-sensitive osmotic swelling of intact, unclamped cells (Suleymanian et al., 1995). Fig. 2 shows that Gd^{3+} also blocked a component of whole-cell current elicited by osmotic swelling and decreased cell volume under perforated patch conditions. E_m was held at −40 mV except during voltage ramps. During the initial 20 min control period in 1T, the I-V relationship was stable (Fig. 2 *A*, curve *a*), and no change in cell volume occurred (Fig. 2 *D*). Exposure of myocytes to 0.6T solution for 5 min increased cell volume by 37 ± 2%, a swelling similar to that previously observed in intact, unclamped rabbit ventricular myocytes (e.g., 34 ± 2%, Drewnowska and Baumgarten, 1991). Both inward current at negative and outward current at positive potentials simultaneously increased in amplitude, at −100 mV from −1.68 ± 0.19 to −7.55 ± 0.21 pA/pF and at +40 mV from +0.74 ± 0.05 to +3.82 ± 0.14 pA/pF (Fig. 2 *A*). After recovery of cell volume and current in 1T solution, the osmotic challenge was repeated in the presence of 10 μM Gd^{3+} (Fig. 2 *B*; 1T, curve *c*; 0.6T, curve *d*). Osmotic swelling still affected membrane currents after Gd^{3+} treatment, but the inward shift of the I-V relationship at negative potentials in 0.6T solution was less pronounced (e.g., from −1.63 ± 0.19 to −3.54 ± 0.18 pA/pF at −100 mV; Fig. 2 *B*). Furthermore, Gd^{3+} decreased the amount of cell swelling significantly; relative cell volume in 0.6T was 1.37 ± 0.02 in the absence of Gd^{3+} and 1.33 ± 0.01 in its presence ($P < 0.05$). The Gd^{3+}-sensitive difference currents in 0.6T and 1T solution are plotted in Fig. 2 *C*. During osmotic stretch in 0.6T solution, Gd^{3+} blocked (Fig. 2 *C*, curves *b* − *d*) an inwardly rectifying current that reversed near −57 mV. Inward rectification also is exhibited by a Gd^{3+}-sensitive cation SAC studied at the single channel level in chick heart (Ruknudin et al., 1993), but other SACs in chick and rat heart have a linear I-V relationship under nearly symmetrical and asymmetrical conditions (Craelius et al., 1988; Ruknudin et al., 1993). In contrast, Gd^{3+} had no effect on currents in 1T (Fig 2 *C*, curves *a* − *c*). This argues that Gd^{3+} blocked only a swelling-induced component of steady state current. Gd^{3+} did not block all of the swelling-induced current, however. The outwardly rectifying component at positive potentials was unaffected (compare Fig. 2, *A* and *B*). The Gd^{3+}-resistant current is likely to be the osmotic swelling-induced anion current, $I_{Cl,swell}$, previously described in atrial, ventricular, and SA nodal myocytes from dog (Tseng, 1992; Sorota, 1992), rabbit (Hagiwara et al., 1992; Duan et al., 1995), rat (Coulombe and Coraboeuf, 1992), guinea pig (Vandenberg et al., 1994; Shuba et al., 1996), and man (Oz and Sorota, 1995; Sakai et al., 1995).

Although intracellular K^+ is controlled by dialysis across the perforated patch, osmotic swelling initially dilutes intracellular K^+ and the resulting shift in I_{K1} might be mistaken for a novel swelling-activated cation current. To test whether I_{K1} contributes to the Gd^{3+}-sensitive current, Ba^{2+}, a potent blocker of I_{K1} in rabbit ventricular myocytes (Giles and Imaizumi, 1988; Shi-

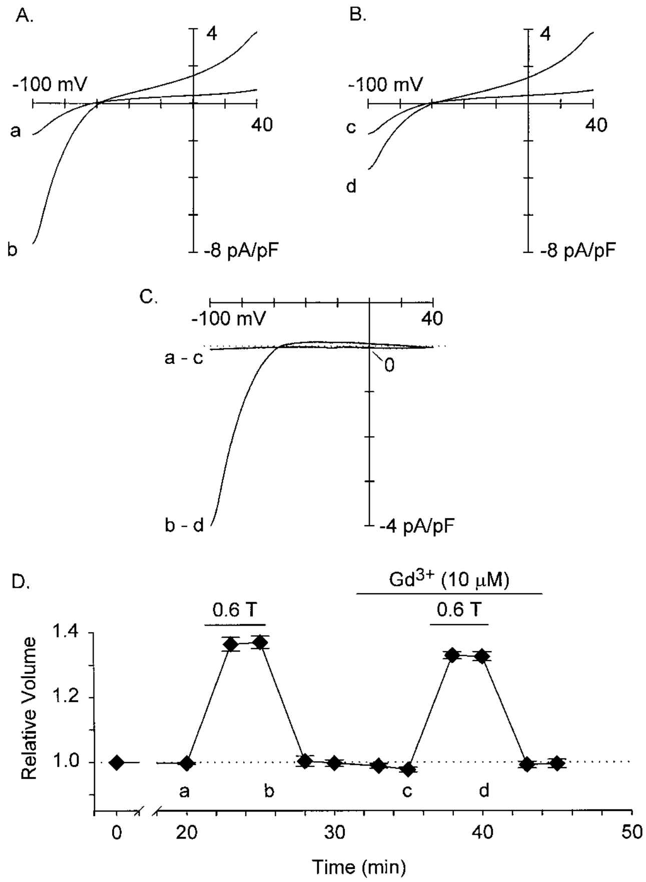

FIGURE 2. Average I-V relationships elicited with voltage ramp in absence (*A*) and presence (*B*) of 10 μM Gd^{3+} under isotonic (1T; *a* and *c*) and hypotonic (0.6T; *b* and *d*) conditions; $n = 13$ cells. (*C*) Gd^{3+}-sensitive difference current in 1T ($a - c$) was negligible (note position of 0 pA/pF); -0.02 ± 0.01 pA/pF at -80 mV, and 0.02 ± 0.01 pA/pF at 0 mV. In 0.6T ($b - d$), the Gd^{3+}-sensitive current was inwardly rectifying, -1.34 ± 0.05 pA/pF at -80 mV and $+0.09 \pm 0.01$ pA/pF at 0 mV, and reversed near -57 mV. (*D*) Cell volumes measured concurrently. Gd^{3+} reduced cell swelling in 0.6T solution. Lower case letters in *D* denote times when I-V curves were obtained. Between ramps, E_h was -40 mV.

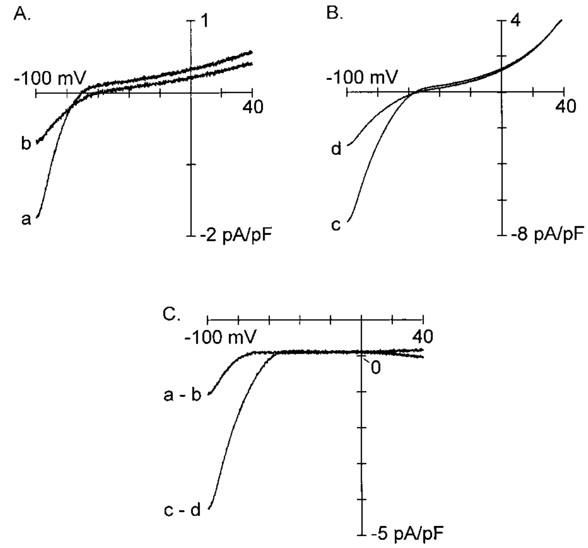

FIGURE 3. Swelling still induced Gd^{3+}-sensitive current after block of I_{K1} by Ba^{2+}. Average I-V relationships in 1T (*A*) in the absence (*a*) and presence (*b*) of 0.2 mM Ba^{2+} and in 0.6T + Ba^{2+} (*B*) in the absence (*c*) and presence (*d*) of 10 μM Gd^{3+}. (*C*) Difference current densities: Ba^{2+}-sensitive current in 1T ($a - b$); Gd^{3+}-sensitive current in 0.6T + Ba^{2+} ($c - d$); $n = 3$ cells. Ba^{2+} did not affect Gd^{3+}-sensitive current (compare Figs. 3 *C*, $c - d$ and 2 *C*, $b - d$). Note change in current scales. E_h, -40 mV; bath, Ca^{2+}-free.

moni et al., 1992), was employed. Under isosmotic conditions, 0.2 mM Ba^{2+} markedly attenuated the inward rectification of the whole-cell current at negative potentials attributable to I_{K1} (Fig. 3 *A*).[2] Nevertheless, swelling in 0.6T + Ba^{2+} still turned on an inwardly rectifying current (Fig. 3 *B*, curve *c*) that was blocked by 10 μM Gd^{3+} (Fig. 3 *B*, curve *d*). The magnitude of the swelling-activated, Gd^{3+}-sensitive current in the presence of Ba^{2+}, -4.29 ± 0.30 pA/pF at -100 mV (Fig. 3 *C*, curve $c - d$) was similar to that in the absence of Ba^{2+}, -4.01 ± 0.23 pA/pF (Fig. 2 *C*, curve $b - d$). These data argue that I_{K1} does not significantly contribute to the swelling-activated Gd^{3+}-sensitive current.

Kinetics of Current Activation

The kinetics of current activation also suggested that separate processes contribute to osmotic swelling-induced currents and positive and negative potentials. To examine activation kinetics, I-V relationships were determined every 30 s during swelling in 0.6T and recovery in 1T solutions in the absence and presence of Gd^{3+}. The currents at +40 and -100 mV are plotted in Fig. 4 *A*. As expected from Fig. 2, the current at +40 mV was resistant to Gd^{3+}, whereas the current at -100 mV consisted of nearly equal Gd^{3+}-sensitive and -insensitive components. The kinetics of current activation are shown more clearly in Fig. 4, *B* and *C*, in which the amplitude of swelling-activated current is expressed as a percentage of the maximum swelling-activated current. Upon exposure to 0.6T solution, the inwardly rectifying current at -100 mV activated significantly more rapidly than the outwardly rectifying current at +40 mV (Fig. 4 *B*); the $t_{1/2}$s were 18.7 ± 1.8 and 55.2 ± 3.4 s, respectively ($P < 0.05$). This difference in $t_{1/2}$ was eliminated when the 0.6T osmotic challenge was repeated

[2] I_{K1} current density in 1T, estimated as Ba^{2+}-sensitive current, was less than that recorded by Giles and Imaizumi (1988) and Shimoni et al. (1992) in rabbit ventricular cells. This difference may arise from the methods. They used ruptured rather than perforated patch. Concentrations of inorganic and organic modulators of I_{K1}, including Mg^{2+} and polyamines (Nichols and Lopatin, 1997), are likely to differ. Furthermore, greater cell capacitance, cell diameter, and animal weight suggest the present experiments used older animals or selected a different population of ventricular cells.

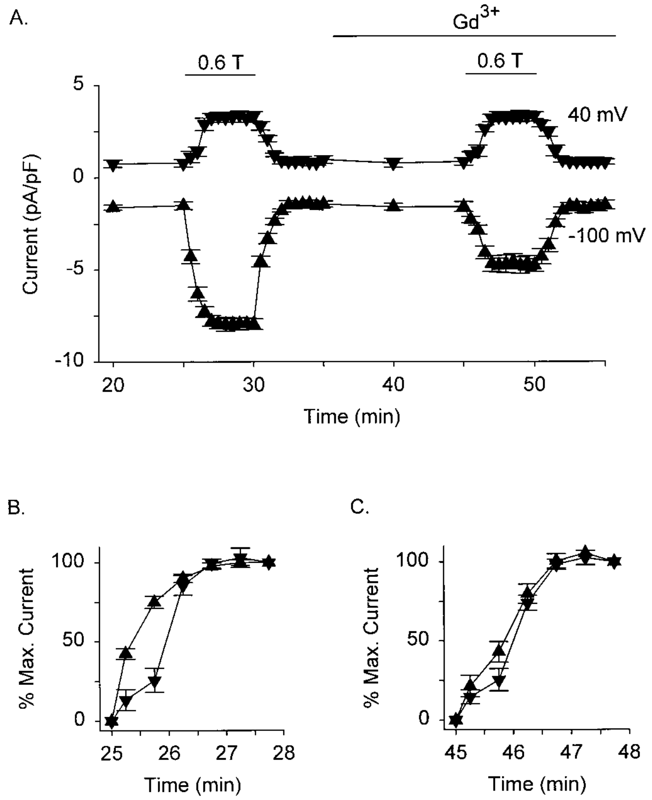

FIGURE 4. Kinetics of activation of current by swelling and inactivation by shrinkage. Ramp clamp protocols were applied every 30 s during swelling in 0.6T and recovery in isotonic 1T in the absence and presence of 10 μM Gd^{3+}. (*A*) Current densities at −100 (▲) and +40 mV (▼); *n* = 4 cells. Time course of current activation in the absence (*B*) and presence (*C*) of Gd^{3+} are compared; current expressed as a percentage of the maximum swelling-induced current. Gd^{3+} significantly increased the $t_{1/2}$ for activation of current at −100 mV (18.7 ± 1.8 vs. 46.3 ± 3.1 s), but did not affect the $t_{1/2}$ at +40 mV. E_h, −40 mV; bath, Ca^{2+}-free.

in the presence of 10 μM Gd^{3+}. Gd^{3+} slowed the $t_{1/2}$ for current activation at –100 mV to 46.3 ± 3.1 s without significantly affecting activation at +40 mV, 53.8 ± 3.5 s; as a result, the $t_{1/2}$s for inward and outward current activation no longer were significantly different ($P > 0.21$). Thus, Gd^{3+} preferentially affected an inwardly rectifying component of osmotic stretch-induced current that activated more rapidly than the rest of the current. Similar results were obtained when the kinetics of current inactivation upon returning the cells to isotonic (1T) solution were considered. Half-times of activation and inactivation are summarized in Table I. Slow activation of swelling-induced outward current was noted previously (Sorota, 1995).

Ionic Nature of Gd^{3+}-sensitive Current

Whereas Gd^{3+} generally is held to be a blocker of cation SACs (Yang and Sachs, 1989; Hamill and McBride, 1996), Robson and Hunter (1994) describe a direct effect of Gd^{3+} on swelling-activated Cl^- currents in *Rana temporaria* proximal tubule cells, and Zhang et al. (1994) and Zhang and Lieberman (1996) describe a Ca^{2+}-dependent indirect effect on swelling-activated Cl^- currents in chick myocytes. The experiments depicted in Fig. 4 were conducted in Ca^{2+}-free bathing media. Nevertheless, the same Gd^{3+}-sensitive and -resistant current components were observed as in the presence of bath Ca^{2+} (see Fig. 2). This argues that swelling-activated currents in mammalian myocytes are not Ca^{2+} dependent (Tseng, 1992; Sorota, 1992; Hagiwara et al., 1992), and we previously showed that the amount of swelling in hypotonic solution is not Ca^{2+} dependent (Suleymanian et al., 1995).

To exclude the possibility that the Gd^{3+}-sensitive current was carried by Cl^-, cells were studied using Cl^--free (methanesulfonate) bath and low Cl^- (aspartate; Cl^- = 5 mM) pipette solutions. The I-V relationships depicted in Fig. 5 *A* were obtained in Cl^--free 1T (Fig. 5 *A*, curve *a*) and 0.6T (Fig. 5 *A*, curve *b*) solutions without Gd^{3+}. Osmotic swelling still increased the current amplitude at negative potentials, but removal of Cl^- sharply attenuated the outwardly rectifying current at positive potentials (see Fig. 2 *A*). The remaining swelling-activated current was blocked almost completely by 10 μM Gd^{3+} (Fig. 5 *B*; Cl^--free 1T, curve *c*; Cl^--free 0.6T, curve *d*). On the other hand, removal of Cl^- had no effect on the Gd^{3+}-sensitive, inwardly rectifying difference current in 0.6T (Fig. 5 *C*, curve *b* − *d*), or on the reduction of cell swelling caused by adding Gd^{3+} to 0.6T solution (Fig. 5 *D*). As before, Gd^{3+} was efficacious only after cell swelling; Gd^{3+} failed to alter either cell volume or the I-V relationship in Cl^--free 1T solution, and the Gd^{3+}-sensitive difference current was negligible (Fig. 5 *C*, curve *a* − *c*). These data suggest that Cl^- contributed to the outwardly rectifying current evoked by hypotonic solution, but was not a significant component of the Gd^{3+}-sensitive, inwardly rectifying current.

If physiologic cations are the major charge carriers of the Gd^{3+}-sensitive, osmotic stretch-activated inward rectifier, removal of Na^+, K^+, and Ca^{2+} from the bath and electrode solutions should markedly attenuate both the inwardly rectifying current in hypotonic solution and

TABLE I
Kinetics of Swelling-induced Current Activation and Inactivation

Condition	Half-times (s) −100 mV	+40 mV
0.6T, activation	18.7 ± 1.3	55.2 ± 2.9
1T, inactivation	18.9 ± 1.5	53.5 ± 2.5
0.6T + Gd^{3+}, activation	46.3 ± 3.2	53.8 ± 2.2
1T + Gd^{3+}, inactivation	47.8 ± 2.8	53.0 ± 3.2

Data from Fig. 4; $t_{1/2}$s for activation by 0.6T and inactivation by 1T solution of inward current at −100 mV and outward current at +40 mV; Gd^{3+}, 10 μM; *n* = 4.

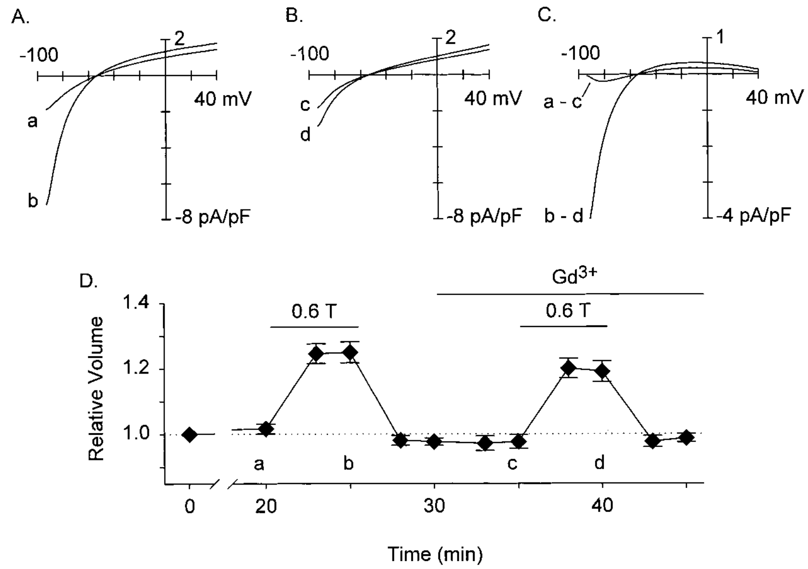

FIGURE 5. Replacement of bath Cl^- with methanesulfonate did not affect Gd^{3+}-sensitive current. Average I-V relationships in Cl^--free 1T (*a* and *c*) and Cl^--free 0.6T (*b* and *d*) solutions in the absence (*A*) and presence (*B*) of 10 μM Gd^{3+}; $n = 5$ cells. Hypotonicity elicited an inwardly rectifying current (*A, b*) that was inhibited by Gd^{3+} (*B, d*). (*C*) Gd^{3+}-sensitive currents under isotonic ($a - c$) and hypotonic ($b - d$) conditions. (*D*) After replacing Cl^-, Gd^{3+} still reduced cell swelling in 0.6T solution. E_h, −40 mV, bath, Cl^--free, Ca^{2+}-free; pipette, low Cl^-.

the Gd^{3+} sensitivity of the remaining current. These predictions were tested by replacing Na^+ and K^+ in the bath with NMDG and in the pipette with Cs^+ and replacing bath Ca^{2+} with Mg^{2+}. Fig. 6 *A* depicts the I-V relationships in 1T, 0.6T, and 0.6T plus Gd^{3+} (Fig. 6 *A*, curves *a–c*, respectively) NMDG solutions. Hypotonic NMDG solution still provoked outwardly rectifying current at positive potentials. As predicted, however, the inward rectifier previously observed at negative potentials was abolished (see Figs. 1 *A* and 5 *A*); instead, the inward current was linear. Moreover, 10 μM Gd^{3+} did not significantly alter the I-V relationship in NMDG-0.6T solution; the negligible Gd^{3+}-sensitive difference current is shown in Fig. 6 *B,* curve $b - c$. Cation replacement also affected the cell volume response. Gd^{3+} no longer reduced cell volume in 0.6T NMDG solution (Fig. 6 *C*; compare Figs. 2 *D* and 5 *D*). These data strongly argue that the inwardly rectifying current induced by osmotic swelling was carried by cations. Therefore, the Gd^{3+}-sensitive current was designated $I_{Cir,swell}$ (cation inward rectifier, swelling activated).

The suggestion that the Gd^{3+}-resistant current elicited by 0.6T solution is $I_{Cl,swell}$ also was supported by experiments in NMDG solutions. Under these conditions, the $I_{Cl,swell}$ blocker 9-AC (1 mM) did not affect the I-V relationship in 1T solution when SACs should be closed (data not shown). On the other hand, 9-AC totally prevented activation of the remaining swelling-induced current in 0.6T NMDG solution (Fig. 6 *A*, curve *d*; compare 1T, curve *a*). The 9-AC–sensitive current (Fig. 6 *B*, curve $c - d$) exhibited outward rectification at positive potentials and a reversal potential (E_{rev}) of -35.6 ± 1.8 mV. Assuming equilibration across the perforated patch, E_{Cl} calculated from the bath and pipette solutions was −32.9 mV after accounting for the effect of ionic strength on activity coefficients ($\gamma_{Cl,bath} = 0.78$; $\gamma_{Cl,cell} = 0.74$). The small difference between E_{rev} and the calculated E_{Cl} is likely to be due in part to imperfect selectivity of stretch-activated anion channels (Tseng, 1992; Sorota, 1992; Hagiwara et al., 1992; Zhang et al., 1993; Vandenberg et al., 1994) and difficulty in controlling intracellular Cl^- with the perforated patch method. Furthermore, Fig. 6 *C* shows that 9-AC signifi-

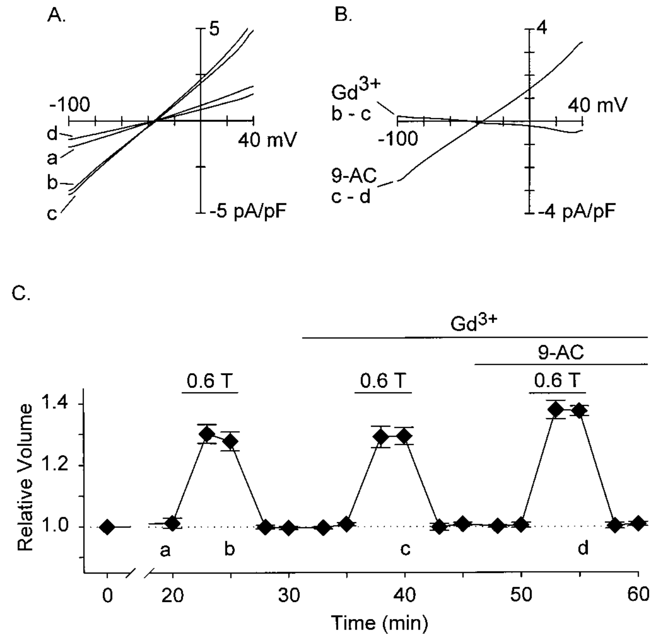

FIGURE 6. Gd^{3+}-sensitive current is cation-dependent. Na^+ and K^+ were replaced with *N*-methyl-D-glucamine and Ca^{2+} with Mg^{2+}. (*A*) Average I-V relationships in 1T (*a*) and 0.6T in the absence (*b*) and presence (*c*) of 10 μM Gd^{3+}, and in 0.6T with Gd^{3+} plus 1 mM 9-AC (*d*); $n = 5$ cells. (*B*) Gd^{3+}-sensitive current ($b - c$) was negligible in 0.6T NMDG solution. In contrast, 9-AC blocked an outwardly rectifying current ($c - d$). (*C*) Gd^{3+} did not affect cell volume in 0.6T NMDG solution, but 9-AC increased swelling. I-V relationships shown in *A* were obtained at times *a–d*. E_h, −40 mV, pipette, Na^+ and K^+ replaced with Cs^+.

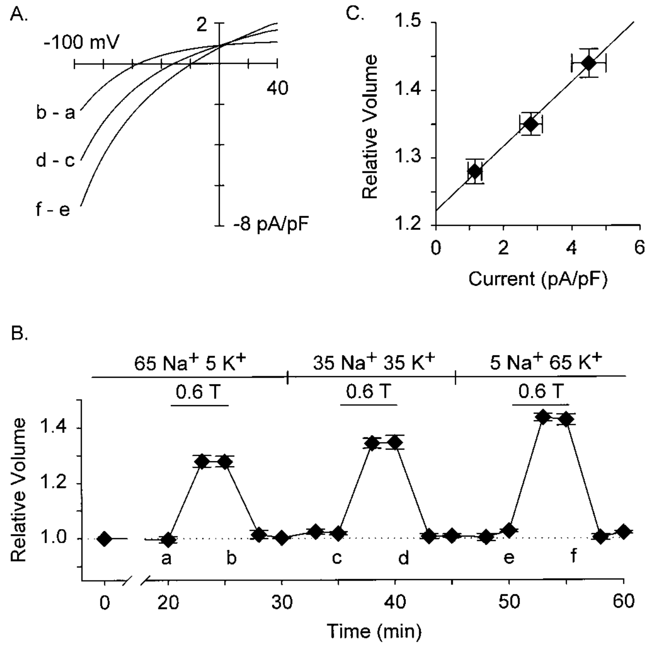

FIGURE 7. Bath K^+ and Na^+ alters swelling-induced cation current and cell volume. (*A*) Average difference currents ($I_{0.6T} - I_{1T}$) obtained in bathing solution containing (mM): 5 K^+, 65 Na^+ (*b* − *a*); 35 K^+, 35 Na^+ (*d* − *c*); and 65 K^+, 5 Na^+ (*f* − *e*); $n = 5$ cells. Although inward rectification was more pronounced, the magnitude of the inward current at diastolic potentials was smaller in 5 mM K^+ than in 35 and 65 mM K^+. (*B*) Concurrent recordings of cell volume. Increasing bath K^+ resulted in greater swelling in 0.6T solution. I-V relationships were measured at times indicated by *a* − *f*. (*C*) Relationship between swelling-induced current at −80 mV and relative cell volume in 0.6T was linear. Summary data for E_{rev}, P_K/P_{Na} ratio, conductance at E_{rev}, and rectifier ratio are presented in Table II. E_h, −40 mV, bath, 0 Cl^- with indicated Na^+ and K^+; pipette, low Cl^-.

cantly increased swelling in 0.6T + Gd^{3+} by 28%, from 1.295 ± 0.011 (Fig. 6 *C*, curve *c*) to 1.377 ± 0.016 (Fig. 6 *C*, curve *d*). A similar effect was noted in intact, unclamped myocytes; in 0.6T without Gd^{3+}, 9-AC increased cell volume 32%, from 1.311 ± 0.019 to 1.413 ± 0.027 (Suleymanian et al., 1995). However, others using the conventional ruptured patch voltage clamp technique failed to detect an acute effect of 9-AC on the volume of swollen myocytes (Tseng, 1992; Sorota, 1992).

The selectivity of $I_{Cir,swell}$ for K^+ and Na^+ was determined next. I-V relationships were recorded in 1T and 0.6T solutions in which the K^+ concentration ($[K^+]_o$) was raised from 5 to 35 and 65 mM by equimolar replacement of Na^+ and Cl^- was replaced by methanesulfonate. The difference currents (0.6T − 1T) are depicted in Fig. 7 *A* ($[K^+]_o$: 5 mM, curve *b* − *a*; 35 mM, curve *d* − *c*; 65 mM, curve *f* − *e*). The E_{rev} and slope conductance at E_{rev} for each condition are presented in Table II. A 13-fold increase of $[K^+]_o$ shifted E_{rev} by 40 mV to more positive voltages and increased the slope conductance 1.5-fold. Also included in Table II are the

TABLE II

Electrophysiological Characteristics of $I_{Cir,swell}$

$[K^+]_o$	$[Na^+]_o$	E_{rev}	P_K/P_{Na}	$g_{Cir,swell}$	Rectifier ratio
mM	*mM*	*mV*		*pS/pF*	
5	65	−56.1 ± 2.3	6.3 ± 0.5	31 ± 2	3.0 ± 0.2
35	35	−31.3 ± 1.9	6.1 ± 0.4	38 ± 3	2.0 ± 0.2
65	5	−19.2 ± 1.3	5.4 ± 0.6	46 ± 3	1.6 ± 0.3

Data from Fig. 7. P_K/P_{Na} ratio was calculated from E_{rev} and ionic concentrations, $g_{Cir,swell}$ from $I_{Cir,swell}$ at E_{rev} ± 10 mV, and rectifier ratio as absolute value of ratio of $I_{Cir,swell}$ at E_{rev} ± 40 mV; $n = 5$.

constant field P_K/P_{Na} ratios calculated from E_{rev} and ion concentrations and the rectifier ratio. For the three combinations of K^+ and Na^+, the P_K/P_{Na} ratio was 5.9 ± 0.3, indicating only a modest selectivity for K^+, and increasing K^+ decreased the extent of rectification by approximately twofold. Because extracellular Na^+ is much greater than K^+ under physiologic conditions, inward current normally would be carried predominantly by Na^+. P_K/P_{Na} ratios of 0.7–7.2 have been estimated for Gd^{3+}-sensitive unitary cation SAC currents elicited in chick ventricle by pipette suction (Bustamante et al., 1991; Ruknudin et al., 1993). The selectivity of the present channel for Ca^{2+} was not examined, although Ca^{2+} is known to permeate cation SACs in a number of tissues, including the heart (Sigurdson et al., 1992).

Replacing Na^+ with K^+ not only altered the difference current, it also caused cell swelling in 0.6T solution to significantly increase from 1.279 ± 0.021 to 1.343 ± 0.018, and 1.428 ±0.020 in 5, 35, and 65 mM $[K^+]_o$ bathing media, respectively. The relationship between the current induced by swelling and cell volume in 0.6T solution is illustrated in Fig. 7 *C*. The data were well described by a straight line with a slope of 0.048 and a y-intercept of 1.22 ($r = 0.99$).

Dose Dependence of Gd^{3+}

Yang and Sachs (1989) reported that 10 μM Gd^{3+} fully blocks stretch-activated cation channels in frog oocytes, but Bustamante et al. (1991) indicated a 10-fold higher dose is necessary in chick and guinea pig myocytes. To characterize the dose dependence of Gd^{3+}s effects on current and volume, cells swollen in Cl^--free 0.6T bath solution were treated with successively higher concentrations of Gd^{3+} (1–30 μM). Fig. 8 *A* shows $I_{Cir,swell}$ (curve *b* − *a*) and the effect of 30 μM Gd^{3+} (curve *f* − *a*). This dose of Gd^{3+} appears to have totally blocked the inward rectifier, leaving a small, nearly linear, swelling-induced current. The residual current is likely to reflect in part the permeation of anions other than Cl^- through the swelling-activated anion channel. The Gd^{3+}-sensitive current in 0.6T solution is depicted in Fig. 8 *B*. As the Gd^{3+} concentration was increased, the amount of current blocked by Gd^{3+} increased significantly ($P < 0.01$).

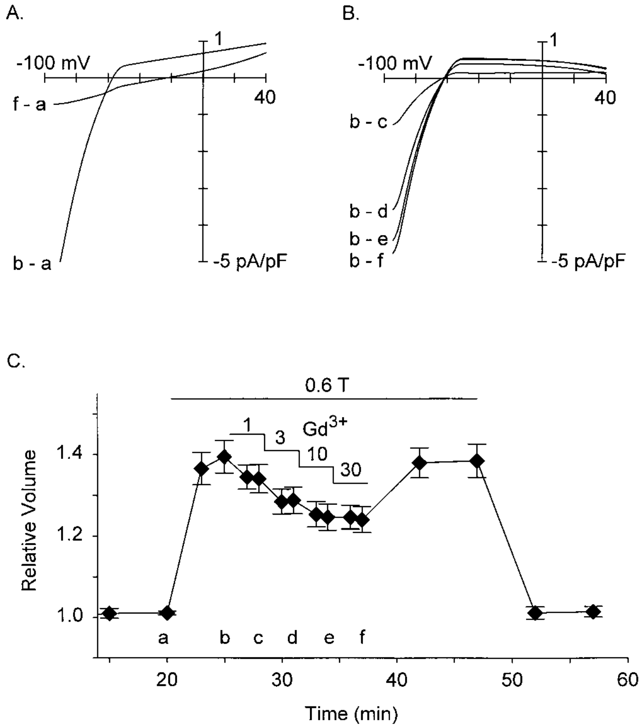

FIGURE 8. Dose dependence of Gd^{3+}-sensitive current. Osmotically swollen cells (*0.6T*) were exposed to successively increasing concentrations of Gd^{3+}, 1–30 μM; $n = 4$ cells. (*A*) Average swelling-induced current ($I_{0.6T} - I_{1T}$; $b - a$) was markedly attenuated by 30 μM Gd^{3+} ($I_{0.6T+Gd} - I_{1T}$; $f - a$). (*B*) Average Gd^{3+}-sensitive currents at four concentrations of Gd^{3+}. (*C*) Concurrent recordings of cell volume. Gd^{3+} caused a dose-dependent shrinkage in 0.6T. Upon washout of Gd^{3+}, cell volume and membrane current return to their initial values. E_h, −80 mV, bath, 0 Cl^-; pipette, low Cl^-.

The effect of Gd^{3+} on cell volume in 0.6T solution also was dose dependent (Fig. 8 *C*). As the Gd^{3+} concentration was increased, relative cell volume in 0.6T solution significantly decreased ($P < 0.001$).

Dose-response curves for current blocked by Gd^{3+} at −80 mV and the reduction of cell volume caused by Gd^{3+} in 0.6T solution are presented in Fig. 9 *A*. The data from Fig. 8, *B* and *C* were fitted to the Hill equation, and the responses are plotted with the fitted maximum taken as 100%. The $K_{0.5}$ and Hill coefficient, n, were: 1.7 ± 0.3 and 1.7 ± 0.4 μM ($r = 0.95$) for block of current (○) and 1.8 ± 0.4 and 1.3 ± 0.2 μM ($r = 0.96$) for the Gd^{3+}-induced cell shrinkage (▲). This means that the 10-μM dose of Gd^{3+} used in other experiments should have blocked 97% of the Gd^{3+}-sensitive current and caused 92% of the maximum volume change.

The excellent correlation between the effects of Gd^{3+} on current and volume are emphasized in Fig. 9 *B*, in which responses were expressed as a percentage of the maximum. The relationship was well described by a straight line with a slope 0.87 and a y-intercept of 8.6%

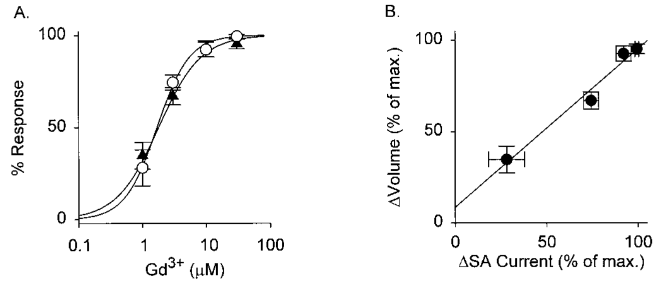

FIGURE 9. Comparison of Gd^{3+}-sensitive current and Gd^{3+}-induced volume changes. Data from Fig. 8 replotted with response (R) expressed as a percentage of maximum response (R_{max}; 30 μM Gd^{3+}). (*A*) Fit of dose-response relationships for block of current (○) and reduction of volume (▲) to Hill equation: $(R/R_{max})\,100\times = C^n/(K' + C^n)$, where C is the Gd^{3+} concentration, n is the Hill coefficient, K' is the apparent constant, and $K_{0.5}$ equals $(K')^{1/n}$. $K_{0.5}$ and n for current and cell volume were 1.7 ± 0.3 μM and 1.7 ± 0.4, and 1.8 ± 0.4 μM and 1.3 ± 0.2, respectively. (*B*) Relationship between block of current and reduction of cell volume was linear.

($r = 0.98$). The slope and y-intercept were not significantly different than 1 and 0, respectively.

Graded Activation of Gd^{3+} Sensitivity

Gd^{3+}-sensitive cation SAC activity in cell-attached patches is a graded function of the negative pressure applied to the pipette and the degree of membrane stretch (Guharay and Sachs, 1984; Sigurdson et al., 1987). For a range of stimuli, the open probability of the nonselective cation mechanoelectrical transduction channel in the bullfrog saccular hair cell has been postulated to be linearly related to membrane tension (Howard et al., 1988), whereas Guharay and Sachs (1984) postulated that gating of the cation SAC in tissue-cultured embryonic chick skeletal muscle cells varies with the square of membrane tension. One might expect the magnitude of $I_{Cir,swell}$ and Gd^{3+}-induced volume changes also would depend on the amount of swelling-induced membrane stretch. To test this idea, myocytes were placed in a series of hypotonic (0.6–0.9T), isotonic (1T), and hypertonic (1.5T) solutions, and the I-V relationship and relative cell volume were monitored. $I_{Cir,swell}$ was measured as the difference between the I-V relationships ± 10 μM Gd^{3+} in each of the superfusates. Fig. 10 *A* shows that Gd^{3+} did not affect membrane current in isotonic solution or when myocytes were shrunken in 1.5T solution. On the other hand, as bath solution osmolarity was gradually stepped from 1 to 0.6T, $I_{Cir,swell}$ increased in a graded fashion. At the same time, osmotic swelling in the presence of Gd^{3+} was attenuated (Fig. 10 *B*). These effects are summarized in Fig. 10 *C* where Gd^{3+}-sensitive current and cell shrinkage are plotted versus bath osmolarity.

Because activation of $I_{Cir,swell}$ should depend on cell volume rather than osmolarity per se, Gd^{3+}-sensitive

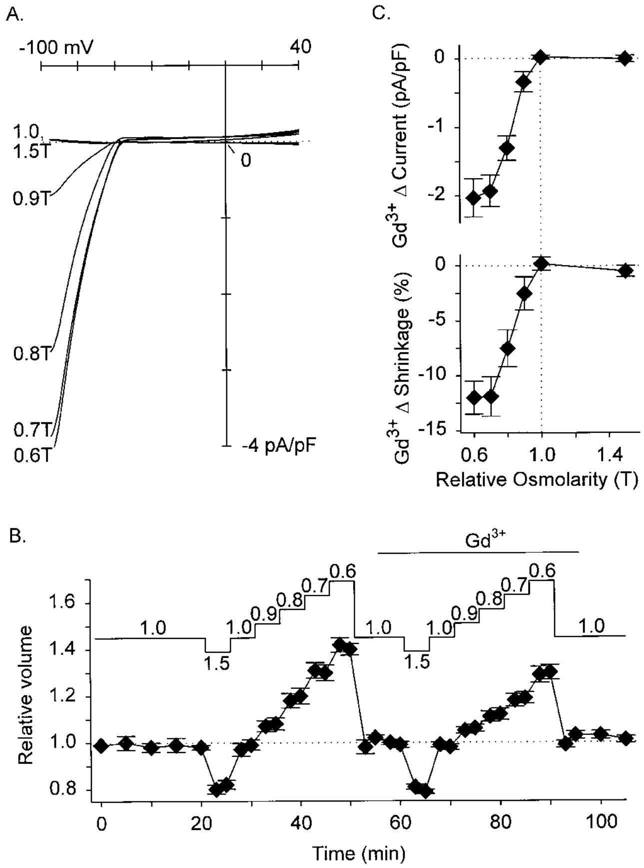

FIGURE 10. Response to Gd^{3+} depends on bath osmolarity. I-V relationships and cell volumes were determined in the absence and presence of 10 μM Gd^{3+} in 0.6T–1.5T bath solutions, $n = 5$ cells. (*A*) Average Gd^{3+}-sensitive currents. (*B*) Cell volumes in the absence and presence of Gd^{3+}; cell volumes in hypotonic solution were reduced by Gd^{3+}. Both the Gd^{3+}-sensitive current and the Gd^{3+}-induced reduction of volume progressively increased as bath osmolarity was decreased; maximum responses were observed in ≤0.7T. In contrast, Gd^{3+} did not alter the I-V relationship or cell volume in isotonic (1T) or hypertonic (1.5T) solutions. (*C*) Gd^{3+}-sensitive current and cell shrinkage are plotted as a function of bath-relative osmolarity. E_h, −80 mV; bath, 0 Cl^-; pipette, low Cl^-.

current at −80 mV and Gd^{3+}-induced cell shrinkage are plotted as a function of relative cell volume before adding Gd^{3+} in Fig. 11, *A* and *B*. Both effects of Gd^{3+} were apparent in 0.9T solution at a relative volume of 1.075 ± 0.025, the smallest amount of swelling examined, and were fully activated in 0.7T solution at a relative volume of 1.305 ± 0.033. Decreasing bath osmolarity to 0.6T did not alter the responses to Gd^{3+} despite causing additional cell swelling. Furthermore, the Gd^{3+}-sensitive current and shrinkage, expressed as a percentage of the maximum Gd^{3+}-induced change, were proportional over a wide range of osmolarities (0.6–1.5T). This linear relationship (Fig. 11 *C*) suggests a tight coupling between the processes.

Kinetics of Gd^{3+}'s Effects on Current and Volume

The data in Figs. 9 *B* and 11 *C* establish that block of current by Gd^{3+} and cell shrinkage are linearly related. It is unclear, though, whether block of current causes cell shrinkage or whether the primary effect of Gd^{3+} is cell shrinkage, which in turn is responsible for the diminution of current. This question can be addressed by examining the kinetics of the two effects. Fig. 12 depicts whole-cell current at −80 mV (○) and cell volume (▲) at 20-s intervals during osmotic swelling and exposure to 10 μM Gd^{3+}. Gd^{3+} decreased the inward current with a $t_{1/2}$ of 50.3 ± 2.5 s (Fig. 12, *down arrow*), whereas the Gd^{3+}-induced cell shrinkage was significantly slower, with a $t_{1/2}$ of 116.3 ± 3.4 s (*up arrow*). These data argue that the primary effect of Gd^{3+} is block of $I_{Cir,swell}$ rather than cell shrinkage. They do not, however, rule out the possibility that cell shrinkage secondary to block of current leads to a further reduction of $I_{Cir,swell}$.

Voltage Dependence of the Sensitivity of Cell Volume to Gd^{3+}

Gd^{3+}-sensitive $I_{Cir,swell}$ was larger at physiologically relevant diastolic potentials than at plateau voltages. At −80 mV, for example, the Gd^{3+}-sensitive current was >2 pA/pF in 0.6T solution (Fig. 10 *A*). A sustained current of this magnitude represents a significant transmembrane ion flux and could cause significant alterations in intracellular osmolarity and, thus, cell volume. Because of its inward-going rectification, however, the Gd^{3+}-sensitive current should have little effect on cell volume at more positive potentials. To investigate this idea, E_h was varied from −80 and −40 mV under isosmotic conditions (1T) and during hyposmotic cell swelling (0.6T) in the absence and presence of 10 μM

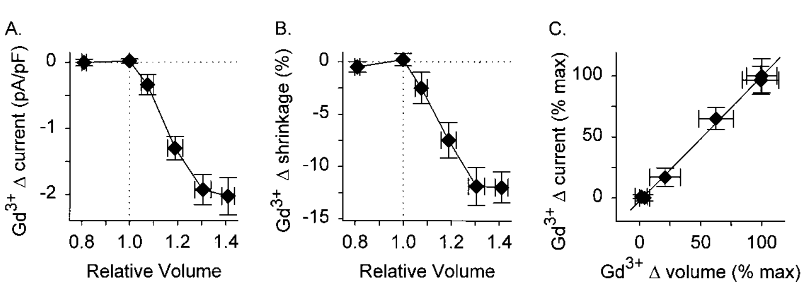

FIGURE 11. Response to Gd^{3+} depends on cell volume. Data taken from Fig. 10. (*A*) Gd^{3+}-sensitive current at −80 mV and (*B*) Gd^{3+}-induced cell shrinkage are plotted as functions of relative cell volume before adding Gd^{3+} (volumes normalized to control, 1T). Maximum responses to Gd^{3+} were observed when relative cell volume was 1.305 ± 0.033 in 0.7T solution. (*C*) Gd^{3+} block of current and Gd^{3+}-induced reduction of cell volume were linearly related.

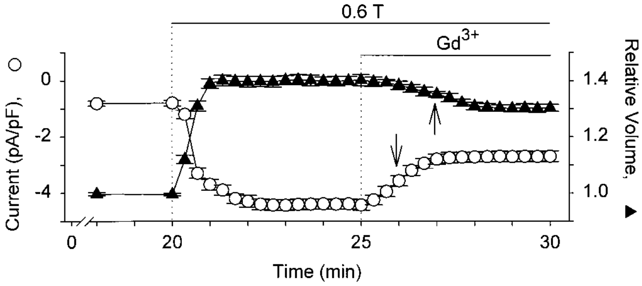

FIGURE 12. Time course of Gd^{3+}-induced reduction of $I_{Cir,swell}$ and volume of osmotically swollen cells. Current at −80 mV (○) and relative cell volume (▲) were monitored and recorded every 20 s in four cells that were swollen in 0.6T hypotonic solution, and then exposed to 10 μM Gd^{3+} in 0.6T. On exposure to Gd^{3+}, reduction of cell volume lagged behind block of current by ∼1 min; $t_{1/2}$s are denoted by arrows. Bath, 0 Ca^{2+}.

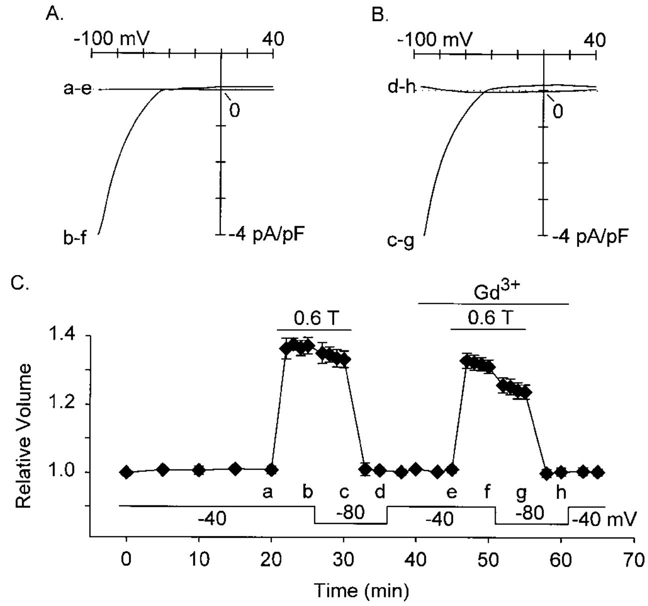

FIGURE 13. Voltage dependence of effect of 10 μM Gd^{3+} on cell volume. E_h was switched between −40 and −80 mV, and I-V relationship and cell volume were measured; n = 4 cells. Average Gd^{3+}-sensitive difference current in 1T (*a* − *e* and *d* − *h*) and 0.6T (*b* − *f* and *c* − *g*) with E_h at −40 (*A*) or −80 (*B*) mV. As expected, Gd^{3+}-sensitive currents were independent of E_h. (*C*) In contrast, Gd^{3+} caused a greater reduction in cell volume when E_h was −80 than when it was −40 mV. Times of switching E_h and recording I-V curves (*a–h*) are indicated in *C*. Bath, 0 Ca^{2+}.

Gd^{3+}. The I-V relationships for the Gd^{3+}-sensitive current holding at −40 mV (Fig. 13 *A*; 1T, curve *a* − *e*; 0.6T, curve *b* − *f*) and at −80 mV (Fig. 13 *B*; 1T, curve *d* − *h*; 0.6T, curve *c* − *g*) are plotted. As expected, the Gd^{3+}-sensitive current in 0.6T was not affected by E_h. Relative cell volume during the protocol is shown in Fig. 13 *C*. If Gd^{3+} blocks an inwardly rectifying cation current, cell volume in 0.6T plus Gd^{3+} should be less than in 0.6T without Gd^{3+} at −80 mV (see Fig. 13 *C*, *c* and *g*), but because depolarization limits the current, Gd^{3+} should fail to alter cell volume at −40 mV (see Fig 13 *C*, *b* and *f*). Both of these predictions were observed. The Gd^{3+}-sensitive current was not the only mechanism regulating volume under these conditions, however. Hyperpolarization from −40 to −80 mV in 0.6T without Gd^{3+} should lead to the activation of inward current and cell swelling at −80 mV if this current acted alone. Instead, a very small cell shrinkage was observed (see Fig. 13 *C*, *b* and *c*). This suggests that the osmotic effect of Gd^{3+}-sensitive cation influx was opposed by a voltage-dependent efflux of osmolytes. When the cation influx was blocked by Gd^{3+}, a significant shrinkage was unmasked on hyperpolarization (see Fig. 13 *C*, *f* and *g*). These portions of data can be explained by the contribution of $I_{Cl,swell}$ to osmolyte fluxes.

DISCUSSION

Osmotic swelling of rabbit ventricular myocytes caused the graded activation of $I_{Cir,swell}$, a Gd^{3+}-sensitive cation current with a P_K/P_{Na} ratio of ∼6. $I_{Cir,swell}$ was not detectable under isosmotic conditions, but was readily measured after a swelling of only 7.5%, the smallest perturbation explored. The I-V relationship for $I_{Cir,swell}$ revealed a strong inward-going rectification and was insensitive to Ba^{2+}, a blocker of I_{K1}. This swelling-induced current appeared to be time independent at potentials negative to 0 mV. Several lines of evidence indicate that $I_{Cir,swell}$ modulates cell volume at physiologically relevant potentials. (*a*) A linear relationship was found between the amount of $I_{Cir,swell}$ blocked by Gd^{3+} during graded osmotic swelling and with varying concentrations of Gd^{3+} and the subsequent Gd^{3+}-induced reduction of cell volume. In 0.6T, 10 μM Gd^{3+} reduced swelling by ∼30%, and Gd^{3+}-induced block of $I_{Cir,swell}$ preceded Gd^{3+}-induced cell shrinkage by ∼1 min. (*b*) Elimination of the Gd^{3+}-sensitive current in hypotonic solution containing NMDG instead of Na^+ and K^+ also eliminated the effect of Gd^{3+} on cell volume. (*c*) The amount of swelling in hypotonic solution was linearly related to $I_{Cir,swell}$ when bath Na^+ was partially replaced by K^+. (*d*) Gd^{3+} also reduces cell volume in osmotically swollen, unclamped myocytes (Suleymanian et al., 1995). These data indicate that osmotic swelling elicited a cation influx via a poorly selective channel. Rather than provoking an RVD, the influx of cations contributed to cell swelling.

A number of studies in mammalian myocytes focused on a swelling-induced, outwardly rectifying anion current, $I_{Cl,swell}$ (Tseng, 1992; Sorota, 1992, 1995; Hagiwara et al., 1992; Coulombe and Coraboeuf, 1992; Vandenberg et al., 1994; Duan et al., 1995; Shuba et al., 1996), and the characteristics of the 9-AC–sensitive $I_{Cl,swell}$ observed here were consistent with these reports. However, in-sensitivity to Gd^{3+} and to omission of extracellular Ca^{2+} distinguishes $I_{Cl,swell}$ in rabbit from that found in chick heart (Zhang et al., 1994). Although previous reports suggested that brief pharmacological blockade of $I_{Cl,swell}$ does not affect cell volume (Tseng, 1992; Sorota, 1992), the present paradigm detected a 28% augmentation of cell swelling in hypotonic solution on blocking $I_{Cl,swell}$ with 9-AC, and the effect of 9-AC on cell volume under voltage clamp was similar to that observed in unclamped myocytes (Suleymanian et al., 1995). A 9-AC–induced swelling was expected because inward current carried by $I_{Cl,swell}$ at diastolic potentials represents the efflux of anions. It is uncertain why we observed increased swelling with 9-AC, whereas others did not. Species differences cannot be ruled out. For example, 9-AC (1 mM) blocks only 50–60% of $I_{Cl,swell}$ in canine and guinea pig myocytes (Tseng, 1992; Sorota, 1994; Vandenberg et al., 1994), but it blocked all of $I_{Cl,swell}$ in rabbit ventricular (Fig. 6 *A*, *a* and *d*) and atrial (Hagiwara et al., 1992) myocytes. In addition, the use of ruptured patch technique (Tseng, 1992; Sorota, 1992) may have blunted changes in intracellular osmolarity caused by 9-AC. Finally, the present digital video microscopy technique for estimating volume has a much greater resolution than measurements of cell width with an ocular reticle (Tseng, 1992; Sorota, 1992).

Basis for the Gd^{3+}-sensitive Swelling-activated Cation Current

This appears to be the first description at the whole-cell level of a Gd^{3+}-sensitive, poorly selective cation current elicited by swelling cardiac myocytes. Single channel recordings from chick, guinea pig, and rat cardiac cells demonstrate that several different cation channels activated by pipette suction are blocked by Gd^{3+} (Bustamante et al., 1991; Sadoshima et al., 1992, Ruknudin et al., 1993). A 25-pS channel in chick heart exhibits strong inward-going rectification that is unaffected by switching Na^+ and K^+ on one side (Ruknudin et al., 1993). In contrast, the rectification found here was markedly diminished when bath Na^+ was replaced by K^+ (Fig. 7 *A*). Other Gd^{3+}-sensitive cation and K^+ channels in chick (Ruknudin et al., 1993) and rat (Sadoshima et al., 1992) have linear unitary I-V relationships in both symmetrical K^+ solutions and with Na^+ replacing K^+ on one side, and the voltage dependence of their open probability would not generate inward rectification of whole-cell currents. Thus, none of the Gd^{3+}-sensitive SACs described at the single channel level can fully account for the behavior of $I_{Cir,swell}$. Nevertheless, the apparent $K_{0.5}$ for block of current and for Gd^{3+}-induced cell shrinkage, 1.7 and 1.8 μM, and Hill coefficients of 1.7 and 1.3, were consistent with Gd^{3+} block of SACs in *Xenopus* oocytes (Yang and Sachs, 1989). Yang and Sachs (1989) suggested that low concentrations of Gd^{3+} screen negative charges near the vestibule of the channel and interact with an allosteric site outside the membrane field to induce a short-lived closed state, whereas higher concentrations cause a cooperative transition to a long-lived closed state.

At positive potentials, an increasing component of outward current also was observed during swelling (Fig. 1 *C*) and attributed to $I_{Cl,swell}$ because of its sensitivity to 9-AC and Cl^- replacement. Swelling-activated outward current may reflect in part a stimulation of the delayed rectifier, I_K, that previously was noted during both osmotic and hydrostatic swelling of guinea pig ventricular myocytes (Sasaki et al., 1992; 1994; Rees et al., 1995; Wang et al., 1996). Both groups agree that swelling primarily increases the slowly activating component, I_{Ks}, but the rapidly activating component, I_{Kr}, is said to either decrease (Rees et al., 1995) or increase (Wang et al., 1996). It is possible that swelling-activated delayed rectifier contributes to the total current in 0.6T, although this current is much smaller in rabbit ventricle than in several other species (Giles and Imaizumi, 1988). The time-dependent current observed here was found at potentials more appropriate for I_{Ks}, although its approaching steady state within 500 ms was suggestive of I_{Kr}. To the extent I_K contributes to swelling-induced current, it also might contribute to the Gd^{3+}-sensitive current. I_{Kr} is blocked by ≥1 μM of another lanthanide, La^{3+}, and ≥10 μM La^{3+} shifts I_{Ks} activation in a positive direction (Sanguinetti and Jurkiewicz, 1990). On the other hand, no component of current attributable to block of I_{Kr} or I_{Ks} by Gd^{3+} was present at appropriate voltages.

Cell swelling or mechanical stretch also has been reported to activate Gd^{3+}-insensitive, poorly selective, cation channels in neonatal rat atrial cells (Kim, 1993; Kim and Fu, 1993). Such channels did not appear to be present in adult rabbit ventricular cells. As judged by the effect of replacement of Na^+ and K^+ with NMDG and Ca^{2+} with Mg^{2+} in Cl^--free solution (Fig. 6, *A* and *B*), all of the swelling activated cation current was blocked by Gd^{3+}. Furthermore, the strong inward rectification of $I_{Cir,swell}$ argues against the participation of free fatty acid–activated (Kim, 1992) or ATP-sensitive (Van Wagoner, 1993) K^+ channels in the response to cell swelling. Activation of either of these channels should have elicited a significant outward cation current in 5 mM $[K^+]_o$, but virtually none was observed.

Osmotic swelling may or may not be equivalent to mechanical stretch or localized membrane deformation as a stimulus for activating SACs (Vandenberg et al., 1996). Although both osmotic swelling and mechanical stimuli distort the membrane and cytoskeleton, osmotic swelling also dilutes intracellular ions and macromolecules. Dilution of the intracellular contents can modulate ion transport by multiple mechanisms

(Baumgarten and Feher, 1998). In particular, reduction of the intracellular K^+ concentration, $[K^+]_i$, (Fozzard and Lee, 1976) raises an important concern for the present study: is $I_{Cir,swell}$ simply a manifestation of dilution of $[K^+]_i$ and the resulting positive shift of E_K on I_{K1}? This is unlikely because Ba^{2+}, a blocker of I_{K1} in rabbit ventricular myocytes (Giles and Imaizumi, 1988; Shimoni et al., 1992), did not inhibit $I_{Cir,swell}$ (Fig. 3), whereas $I_{Cir,swell}$ was blocked by Gd^{3+}, which did not affect the background currents, including I_{K1} in 1T (Fig. 2). Moreover, osmotic dilution of $[K^+]_i$ is transient under patch clamp conditions. By the time I-V curves were recorded, at least 5 min after the onset of an osmotic challenge, dialysis of the cytoplasm by the patch pipette should have substantially reduced changes in $[K^+]_i$. Sasaki et al. (1994) found that I_{K1} was hardly affected only 2 min after exposing dialyzed myocytes to 0.7T solution. Despite these compelling arguments that swelling-induced shifts in E_K cannot fully explain the data, the possibility remains that cellular dialysis did not completely restore $[K^+]_i$ after an osmotic challenge. Such incomplete dialysis, to the extent that it occurred, could have affected characterization of $I_{Cir,swell}$.

Gd^{3+}-sensitive Current Alters Cell Volume

In response to graded osmotic swelling, equimolar partial replacement of bath Na^+ with K^+, and varying the concentration of Gd^{3+}, the magnitude of the cation current blocked by Gd^{3+} at −80 mV was linearly related to the ensuing reduction of cell volume. Also, Gd^{3+}'s effect on $I_{Cir,swell}$ preceded its effect on cell volume. Although these data imply that $I_{Cir,swell}$ modulates cardiac cell volume, a more quantitative comparison may be helpful. To estimate the expected volume change, the Gd^{3+}-sensitive current was integrated over time and converted to changes in intracellular molarity. Table III shows the result of calculations based on the experiments depicted in Fig. 13 in which E_h was set at −80 and −40 mV and analogous studies switching E_h between −40 and 0 mV. A much greater Gd^{3+}-sensitive cation influx occurred when myocytes were held at −80 mV than at −40 or 0 mV or during the voltage ramp. The integral of $I_{Cir,swell}$ accounted for a 16.2 ± 1.2 mM change in concentration at −80 mV, ~25× more than at −40 or 0 mV. This amounted to a 5.5% decrease in osmolarity, whereas volume decreased ~7% at −80 mV.

An additional issue complicates the quantitative relationship between ionic currents under voltage clamp and cell volume changes. There is also a flux between the pipette and cell, and the pipette transport numbers for cations, t^+, and anions, t^-, must be considered, as is illustrated in Fig. 14. If the membrane and patch pipette are both perfectly selective for cations or anions, the ion flux between the pipette and cell will exactly balance the transmembrane ion flux and no volume

TABLE III
Effect of Gd^{3+}-sensitive Current on Intracellular Concentrations

Parameter	Holding potential −80 mV	−40 mV	0 mV
Q_{RAMP} (nC)	−3.5 ± 0.3	−3.3 ± 0.2	−3.3 ± 0.2
Q_{HOLD} (nC)	−59.2 ± 2.3	+0.4 ± 0.1	+0.8 ± 0.2
Q_{TOTAL} (nC)	−62.7 ± 2.4	−2.9 ± 0.3	−2.5 ± 0.3
Mole equivalent (fmol)	−650 ± 25	−29.9 ± 2.6	−25.9 ± 2.7
Cell volume (pL)	40.1 ± 2.1	43.3 ± 2.3	42.4 ± 2.0
ΔMolarity (mM)	−16.2 ± 1.2	−0.7 ± 0.1	−0.6 ± 0.1

Data from Fig. 13 and other experiments where E_h was varied between −40 and 0 mV (data not shown). Q_{RAMP}, Gd^{3+}-sensitive current integrated over five ramps (total time of each ramp protocol = 10 s) done at 1-min intervals during exposure to 0.6T solution; Q_{HOLD}, Gd^{3+}-sensitive current at E_h; $Q_{TOTAL} = Q_{RAMP} + Q_{HOLD}$. Cell volume calculated assuming cylindrical geometry. n = 4, 8, and 4 at −80, −40, and 0 mV, respectively.

change will occur. The other extreme assumes the pipette and membrane have opposite cation/anion selectivity. In such a case, total fluxes into or out of the cell are exactly twice the transmembrane flux, and observed volume changes are exactly twice those expected from transmembrane currents. The optimal situation is for the pipette cation and anion transport numbers both to equal 0.5. In that case, cation and anion fluxes between the pipette and cell are equal in magnitude but opposite in direction, and their effects on cell volume cancel. As a result, the observed volume change will exactly equal the change expected from the measured ionic current.

Unfortunately, the transport numbers of a perforated patch are difficult to predict. The fluxes are determined by the combined characteristics of the poreformer and native membrane channels. Amphotericin pores are permeant to both monovalent cations and anions (Marty and Finkelstein, 1975; Horn and Marty, 1988; Ebihara et al., 1995; Kyrozis and Reichling, 1995), and amphotericin may affect the properties of native channels (Hsu and Burnette, 1993). In preliminary studies, P_K/P_{Cl} of amphotericin-treated myocytes was estimated as 0.8–0.9 (see METHODS). Using P_K/P_{Cl} to approximate P_{cation}/P_{anion} and taking the potential across the perforated patch as ~0 mV, t^+ was ~0.44–0.47. Although only an approximation, these data suggest that the cation and anion fluxes between pipette and cell were roughly comparable and, therefore, that cell volume changes measured under perforated patch conditions should approximate those expected from the measured ionic currents.

Physiological and Pathophysiological Implications

Activation of $I_{Cir,swell}$ and $I_{Cl,swell}$ may directly affect cardiac electrical activity, alter ionic gradients, and con-

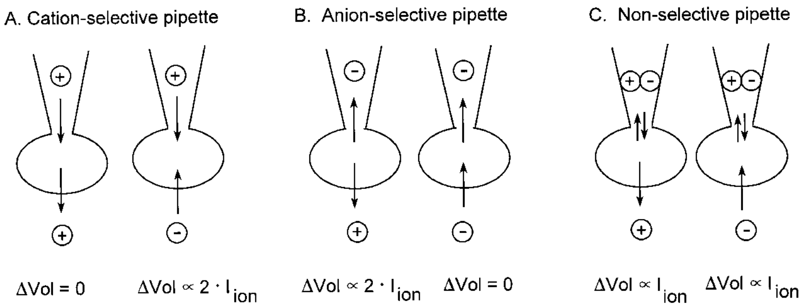

FIGURE 14. Illustration of effect of pipette transport numbers for cations (t^+) and anions (t^-) on cell volume changes under voltage clamp. Cell volume is altered by both transmembrane current (I_{ion}) and current flowing between the pipette and cell. Arrows represent fluxes of osmotic equivalents generated by an outward I_{ion} carried by either a cation efflux or anion influx. For a perfectly cation-selective (*A*; $t^+ = 1$, $t^- = 0$) or anion-selective (*B*; $t^+ = 0$, $t^- = 1$) pipette, no volume change will occur if the selectivity of the membrane and pipette are the same, and twice the volume change expected from I_{ion} will occur if the selectivities are opposite. For a nonselective pipette (*C*; $t^+ = 0.5$, $t^- = 0.5$), cation and anion fluxes between the pipette and cell always cancel exactly, and volume changes will be precisely those expected from I_{ion}.

tribute to cell volume regulation. These currents are likely to be activated during ischemia and reperfusion (Reimer and Jennings, 1992) and surgical cardioplegia (Drewnowska et al., 1991; Handy et al., 1996) when myocyte swelling is pronounced. The present studies do not establish whether cell swelling is the required stimulus or if stretch also activates the same channels. However, several effects of stretch are blocked by Gd^{3+} and are consistent with activation of $I_{Cir,swell}$ by stretch. For example, 10 μM Gd^{3+} blocks stretch-induced depolarizations and ventricular premature beats initiated by rapid inflation of a ventricular balloon in canine ventricle (Hansen et al., 1991; Stacy et al., 1992), 80 μM Gd^{3+} blocks stretch-induced delayed afterdepolarizations, premature beats, and poststretch augmentation of contractile force in rat atria (Tavi et al., 1996), and 5 μM Gd^{3+} decreases stretch-induced release of atrial natriuretic peptide from rat atrium (Laine et al., 1994). Furthermore, infusion of $GdCl_3$ (76 μmol/kg) attenuates the upward shift of the left ventricular diastolic pressure–volume relationship caused by pacing-induced cardiac ischemia in dogs (Takano and Glantz, 1995). Another intriguing possibility is the involvement of stretch-activated channels in congestive heart failure. We found that $I_{Cir,swell}$ was chronically activated in isosmotic solution in ventricular myocytes from dogs with pacing-induced congestive failure (Clemo et al., 1995). Thus, activation of $I_{Cir,swell}$ by cell swelling or mechanical stretch may have important implications for myocyte volume regulation, and electrical and mechanical activity under both physiologic and pathophysiologic conditions.

This work was supported by National Heart, Lung, and Blood Institute grants HL-46764 and HL-02798.

Original version received 3 April 1997 and accepted version received 20 June 1997.

REFERENCES

Baumgarten, C.M., and J.J. Feher. 1998. Osmosis and the regulation of cell volume. *In* Cell Physiology Source Book, 2nd ed. N. Sperelakis, editor. Academic Press, Inc., San Diego, CA. 254–293.

Brezden, B.L., D.R. Gardner, and C.E. Morris. 1986. A potassium-selective channel in isolated *Lymnaea stagnalis* heart muscle cells. *J. Exp. Biol.* 123:175–189.

Bustamante, J.O., A. Ruknudin, and F. Sachs. 1991. Stretch-activated channels in heart cells: relevance to cardiac hypertrophy. *J. Cardiovasc. Pharmacol.* 17(Suppl. 2):110–113.

Clemo, H.F., and C.M. Baumgarten. 1991. Atrial natriuretic factor decreases cell volume of rabbit atrial and ventricular myocytes. *Am. J. Physiol.* 260:C681–C690.

Clemo, H.F., and C.M. Baumgarten. 1995. Gd^{3+} reduces a cation current and cell swelling in osmotically challenged adult rabbit ventricular myocytes. *Biophys. J.* 68:393*a*. (Abstr.)

Clemo, H.F., J.J. Feher, and C.M. Baumgarten. 1992. Modulation of rabbit ventricular cell volume and $Na^+/K^+/2Cl^-$ cotransport by cGMP and atrial natriuretic factor. *J. Gen. Physiol.* 100:89–114.

Clemo, H.F., B.S. Stambler, and C.M. Baumgarten. 1995. Persistent stretch-activated current and cell volume in congestive heart failure. *Circulation.* 92:I–504. (Abstr.)

Coulombe, A., and E. Coraboeuf. 1992. Large-conductance chloride channels of new-born rat cardiac myocytes are activated by hypotonic media. *Pflügers Arch.* 422:143–150.

Craelius, W., V. Chen, and N. el-Sherif. 1988. Stretch activated ion channels in ventricular myocytes. *Biosci. Rep.* 8:407–414.

Doroshenko, P., and E. Neher. 1992. Volume-sensitive chloride conductance in bovine chromaffin cell membrane. *J. Physiol. (Camb.).* 449:197–218.

Drewnowska, K., and C.M. Baumgarten. 1991. Regulation of cellular volume in rabbit ventricular myocytes: bumetanide, chlorothiazide, and ouabain. *Am. J. Physiol.* 260:C122–C131.

Drewnowska, K., H.F. Clemo, and C.M. Baumgarten. 1991. Prevention of myocardial intracellular edema induced by St. Thomas' Hospital cardioplegic solution. *J. Mol. Cell. Cardiol.* 23:1215–1222.

Duan, D., B. Fermini, and S. Nattel. 1995. α-Adrenergic control of volume-regulated Cl^- currents in rabbit atrial myocytes. Characterization of a novel ionic regulatory mechanism. *Circ. Res.* 77: 379–393.

Ebihara, S., K. Shirato, N. Harata, and N. Akaike. 1995. Gramicidin-perforated patch recording: GABA response in mammalian neurones with intact intracellular chloride. *J. Physiol. (Camb.)* 484:77–86.

Fozzard, H.A., and C.O. Lee. 1976. Influence of changes in external potassium and chloride ions on membrane potential and intracellular potassium ion activity in rabbit ventricular muscle. *J. Physiol. (Camb.)* 256:663–689.

Giles, W.R., and Y. Imaizumi. 1988. Comparison of potassium currents in rabbit atrial and ventricular cells. *J. Physiol. (Camb.).* 405: 123–145.

Guharay, F., and F. Sachs. 1984. Stretch-activated single ion channel currents in tissue-cultured embryonic chick skeletal muscle. *J. Physiol. (Camb.).* 352:685–701.

Hagiwara, N., H. Masuda, M. Shoda, and H. Irisawa. 1992. Stretch-activated anion currents of rabbit cardiac myocytes. *J. Physiol. (Camb.).* 456:285–302.

Hall, S.K., J. Zhang, and M. Lieberman. 1995. Cyclic AMP prevents activation of a swelling-induced chloride-sensitive conductance in chick heart cells. *J. Physiol. (Cambr.).* 488:359–369.

Hamill, O.P., and D.W. McBride, Jr. 1996. The pharmacology of mechanogated membrane ion channels. *Pharmacol. Rev.* 48:231–252.

Handy, J.R., Jr., B.H. Dorman, M.J. Cavallo, R.B. Hinton, R.C. Roy, F.A. Crawford, and F.G. Spinale. 1996. Direct effects of oxygenated crystalloid or blood cardioplegia on isolated myocyte contractile function. *J. Thorac. Cardiovasc. Surg.* 112:1064–1072.

Hansen, D.E., M. Borganelli, G.P. Stacy, Jr., and L.K. Taylor. 1991. Dose-dependent inhibition of stretch-induced arrhythmias by gadolinium in isolated canine ventricles. Evidence for a unique mode of antiarrhythmic action. *Circ. Res.* 69:820–831.

Horn, R., and A. Marty. 1988. Muscarinic activation of ionic currents measured by a new whole-cell recording method. *J. Gen. Physiol.* 92:145–159.

Howard, J., W.M. Roberts, and A.J. Hudspeth. 1988. Mechanoelectrical transduction by hair cells. *Annu. Rev. Biophys. Chem.* 17:99–124.

Hsu, S.-F., and R.R. Burnette. 1993. The effect of amphotericin B on the K-channel activity of MDCK cells. *Biochim. Biophys. Acta.* 1152:189–191.

Kim, D. 1992. A mechanosensitive K^+ channel in heart cells. *J. Gen. Physiol.* 100:1021–1040.

Kim, D. 1993. Novel cation-selective mechanosensitive ion channel in the atrial cell membrane. *Circ. Res.* 72:225–231.

Kim, D., and C. Fu. 1993. Activation of a nonselective cation channel by swelling in atrial cells. *J. Membr. Biol.* 135:27–37.

Kinard, T.A., and L.S. Satin. 1995. An ATP-sensitive Cl^- channel current that is activated by cell swelling, cAMP, and glyburide in insulin-secreting cells. *Diabetes.* 44:1461–1466.

Kyrozis, A., and D.B. Reichling. 1995. Perforated-patch recording with gramicidin avoids artifactual changes in intracellular chloride concentration. *J. Neurosci. Methods.* 57:27–35.

Laine, M., O. Arjamaa, O. Vuolteenaho, H. Ruskoaho, and M. Weckstrom. 1994. Block of stretch-activated atrial natriuretic peptide secretion by gadolinium in isolated rat atrium. *J. Physiol. (Camb.).* 480:553–561.

Lambert, I.H., and E.K. Hoffman. 1994. Cell swelling activates separate taurine and chloride channels in Ehrlich mouse ascites tumor cells. *J. Membr. Biol.* 142:289–298.

Marty, A., and A. Finkelstein. 1975. Pores formed in lipid bilayer membranes by nystatin. Differences in its one-sided and two-sided action. *J Gen. Physiol.* 65:515–526.

Morris, C.E. 1990. Mechanosensitive ion channels. *J. Membr. Biol.* 113:93–107.

Neher, E. 1992. Correction for liquid junction potentials in patch clamp experiments. *Methods Enzymol.* 207:123–131.

Nichols, C.G., and N. Lopatin. 1997. Inward rectifier potassium channels. *Annu. Rev. Physiol.* 59:171–191.

Oz, M.C., and S. Sorota. 1995. Forskolin stimulates swelling-induced chloride current, not cardiac cystic fibrosis transmembrane-conductance regulator, in human cardiac myocytes. *Circ. Res.* 75: 1063–1070.

Rae, J., K. Cooper, P. Gates, and M. Watsky. 1991. Low access resistance perforated patch recordings using amphotericin B. *J. Neurosci. Methods.* 37:15–26.

Rasmusson, R.L., D.G. Davis, and M. Lieberman. 1993. Amino acid loss during volume regulatory decrease in cultured chick heart cells. *Am. J. Physiol.* 264:C136–C145.

Rees, S.A., J.I. Vandenberg, A.R. Wright, A. Yoshida, and T. Powell. 1995. Cell swelling has differential effects on the rapid and slow components of delayed rectifier potassium current in guinea pig cardiac myocytes. *J. Gen. Physiol.* 106:1151–1170.

Reimer, K.A., and R.B. Jennings. 1992. Myocardial ischemia, hypoxia, and infarction. *In* The Heart and Cardiovascular System. Scientific Foundations, 2nd ed. H.A. Fozzard, E. Haber, R.B. Jennings, A.M. Katz, and H.E. Morgan, editors. Raven Press, New York. 1875–1973.

Robson, L., and M. Hunter. 1994. Role of cell volume and protein kinase C in regulation of a Cl^- conductance in single proximal tubule cells of *Rana temporaria. J. Physiol. (Camb.).* 480:1–7.

Ruknudin, A., F. Sachs, and J.O. Bustamante. 1993. Stretch-activated ion channels in tissue-cultured chick heart. *Am. J. Physiol.* 264:H960–H972.

Sachs, F. 1988. Mechanical transduction in biological systems. *Crit. Rev. Biomed. Eng.* 16:141–169.

Sackin, H. 1995. Mechanosensitive channels. *Annu. Rev. Physiol.* 57: 333–353.

Sadoshima, J.-I., T. Takahashi, L. Jahn, and S. Izumo. 1992. Roles of mechano-sensitive ion channels, cytoskeleton, and contractile activity in stretch-induced immediate-early gene expression and hypertrophy of cardiac myocytes. *Proc. Natl. Acad. Sci. USA.* 89: 9905–9909.

Sakai, R., N. Hagiwara, H. Kasanuki, and S. Hosoda. 1995. Chloride conductance in human atrial cells. *J. Mol. Cell. Cardiol.* 27:2403–2408.

Sanguinetti, M.C., and N.K. Jurkiewicz. 1990. Lanthanum blocks a specific component of I_K and screens membrane surface charge in cardiac cells. *Am. J. Physiol.* 259:H1881–H1889.

Sasaki, N., T. Mitsuiye, and A. Noma. 1992. Effects of mechanical stretch on membrane currents of single ventricular myocytes of guinea-pig heart. *Jpn. J. Physiol.* 42:957–970.

Sasaki, N., T. Mitsuiye, Z. Wang, and A. Noma. 1994. Increase of the delayed rectifier K^+ and Na^+-K^+ pump currents by hypotonic solutions in guinea pig cardiac myocytes. *Circ. Res.* 75:887–895.

Schwiebert, E.M., J.W. Mills, and B.A. Stanton. 1994. Actin-based cytoskeleton regulates a chloride channel and cell volume in a renal cortical collecting duct cell line. *J. Biol. Chem.* 269:7081–7089.

Shimoni, Y., R.B. Clark, and W.R. Giles. 1992. Role of an inwardly rectifying potassium current in rabbit ventricular action potential. *J. Physiol. (Camb.).* 448:709–727.

Shuba, L.M., T. Ogura, and T.F. McDonald. 1996. Kinetic evidence distinguishing volume-sensitive chloride current from other types in guinea-pig ventricular myocytes. *J. Physiol. (Camb.).* 491: 69–80.

Sigurdson, W.J., C.E. Morris, B.L. Brezden, and D.R. Gardner. 1987. Stretch activation of a K^+ channel in molluscan heart cells. *J. Exp. Biol.* 127:191–209.

Sigurdson, W., A. Ruknudin, and F. Sachs. 1992. Calcium imaging of mechanically induced fluxes in tissue-cultured chick heart: role of stretch-activated ion channels. *Am. J. Physiol.* 262: H1110–H1115.

Sorota, S. 1992. Swelling-induced chloride-sensitive current in canine atrial cells revealed by whole-cell patch-clamp method. *Circ. Res.* 70:679–687.

Sorota, S. 1994. Pharmacologic properties of the swelling-induced chloride current of dog atrial myocytes. *J. Cardiovasc. Electrophysiol.* 5:1006–1016.

Sorota, S. 1995. Tyrosine protein kinase inhibitors prevent activation of cardiac swelling-induced chloride current. *Pflügers Arch.* 431:178–185.

Stacy, G.P., Jr., R.L. Jobe, L.K. Taylor, and D.E. Hansen. 1992. Stretch-induced depolarizations as a trigger of arrhythmias in isolated canine left ventricles. *Am. J. Physiol.* 263:H613–H621.

Sukharev, S.I., P. Blount, B. Martinac, H.R. Guy, and C. Kung. 1996. MscL: a mechanosensitive channel in *Escherichia coli. Soc. Gen. Physiol. Ser.* 51:133–141.

Suleymanian, M.A., and C.M. Baumgarten. 1996. Osmotic gradient-induced water permeation across the sarcolemma of rabbit ventricular myocytes. *J. Gen. Physiol.* 107:503–514.

Suleymanian, M.A., H.F. Clemo, N.M. Cohen, and C.M. Baumgarten. 1995. Stretch-activated channel blockers modulate cell volume in cardiac ventricular myocytes. *J. Mol. Cell. Cardiol.* 27:721–728.

Takano, H., and S.A. Glantz. 1995. Gadolinium attenuates the upward shift of the left ventricular diastolic pressure-volume relation during pacing-induced ischemia in dogs. *Circulation.* 91: 1575–1587.

Tavi, P., M. Laine, and M. Weckström. 1996. Effect of gadolinium on stretch-induced changes in contraction and intracellularly recorded action- and after-potentials of rat isolated atrium. *Br. J. Pharmacol.* 118:407–413.

Tseng, G.N. 1992. Cell swelling increases membrane conductance of canine cardiac cells: evidence for a volume-sensitive Cl channel. *Am. J. Physiol.* 262:C1056–C1068.

Vandenberg, J.I., S.A. Rees, A.R. Wright, and T. Powell. 1996. Cell swelling and ion transport pathways in cardiac myocytes. *Cardiovasc. Res.* 32:85–97.

Vandenberg, J.I., A. Yoshida, K. Kirk, and T. Powell. 1994. Swelling-activated and isoprenaline-activated chloride currents in guinea pig cardiac myocytes have distinct electrophysiology and pharmacology. *J. Gen. Physiol.* 104:997–1017.

Van Wagoner, D.R. 1993. Mechanosensitive gating of atrial ATP-sensitive potassium channels. *Circ. Res.* 72:973–983.

Wang, Z., T. Mitsuiye, and A. Noma. 1996. Cell distention-induced increase of the delayed rectifier K^+ current in guinea pig ventricular myocytes. *Circ. Res.* 78:466–474.

Worrell, R.T., A.G. Butt, W.H. Cliff, and R.A. Frizzell. 1989. A volume-sensitive conductance in human colonic cell line T84. *Am. J. Physiol.* 256:C1111–C1119.

Yang, X.-C., and F. Sachs. 1989. Block of stretch-activated ion channels in *Xenopus* oocytes by gadolinium and calcium ions. *Science (Wash. DC).* 243:1068–1071.

Zhang, J., S.K. Hall, and M. Lieberman. 1994. An early transient current activates the swelling- induced chloride conductance in cardiac myocytes. *Biophys. J.* 66:A442. (Abstr.)

Zhang, J., and M. Lieberman. 1996. Chloride conductance is activated by membrane distention of cultured chick heart cells. *Cardiovasc. Res.* 32:168–179.

Zhang, J., R.L. Rasmusson, S.K. Hall, and M. Lieberman. 1993. A chloride current associated with swelling of cultured chick heart cells. *J. Physiol. (Camb.).* 472:801–820.